Interval Observer Based Sensor Fault Estimation for High-Speed Railway Traction Devices with Disturbances ☆

Yang Tian[a], Ke Zhang[a,*], Bin Jiang[a], Xing-Gang Yan[b]

[a] *School of Automation Engineering, Nanjing University of Aeronautics and Astronautics, 211106 P.R. China*
[b] *School of Engineering and Digital Arts, University of Kent, Canterbury, Kent CT2 7NT, United Kingdom.*

Abstract

In this paper, fault estimation for high-speed railway traction devices with sensor fault and disturbances is investigated based on the interval observer and unknown input observer (IO-UIO). Firstly, the mathematical model of the induction motor d-q coordinate system is introduced. Secondly, the proposed method, which can completely eliminate the external disturbance, is studied based on the disturbance isolation characteristic of the unknown input observer. Then, an interval observer is introduced to deal with the nonlinear part, which sandwiched the actual system between the upper and lower bounds. The Metzler matrix is constructed using an equivalent transformation and through the unified design based on the concept of the augmented state to form a global fault augmented model. Finally, simulation results are presented to illustrate the effectiveness and advantages of the proposed IO-UIO.

Keywords: Railway traction systems, Metzler matrix, Equivalent transformation, Interval observer, Unknown input observer

☆This work was supported in part by the National Natural Science Foundation of China under Grants 61490703 and 61673207.

*Corresponding author
Email addresses: nuaaty@163.com (Yang Tian), kezhang@nuaa.edu.cn (Ke Zhang), binjiang@nuaa.edu.cn (Bin Jiang), x.yan@kent.ac.uk (Xing-Gang Yan)

1. Introduction

The development of high-speed railways and the progress in science and technology over the past decade have resulted in the increased requirements for the safety and stability of high-speed trains. These necessities are closely related to the safety of people's life and property. High-speed railway has developed rapidly in many countries worldwide [1]. At present, the world's most representative high-speed railways include the German ice train, Japan Shinkansen, French TGV trains and Chinese CRH trains. Compared with air transport, the high-speed railway has several advantages, such as low cost, large operating area, environmental protection and all-weather operation. The development of high-speed railway has not only a stimulating effect on equipment technology and modern manufacturing but also presents great impacts on information communication and construction modernisation.

Modern control systems becoming complex. Therefore, fault detection, fault diagnosis and fault-tolerant techniques have received more attention [2–17]. Fault detection is the first step of fault diagnosis, which determines the occurrence of a system fault. The fault should be detected before it becomes serious. Fault isolation is to determine the specific location of the fault. Finally, fault estimation is performed to identify the form and size of the fault and is an important prerequisite for fault tolerance control. However, the quality of actuators and sensors in a control system has been deteriorating with time. Moreover, the system sensors are used to measure system output, and these sensors indirectly affect the performance of the control system. the fault detection and diagnosis (FDD) and fault tolerance of the actuator faults are easier to determine than sensor faults (i.e. [18–20]). Only a few studies have reported on the FDD of sensor faults.

Traction motor is the core equipment of high-speed trains, and this part is closely related to the safe operation of the train. Safety of the traction motor becomes very important as the high-speed train accelerates. Therefore, investigating the fault diagnosis of a traction motor is of great practical significance.

Induction motors play an important role in the industry. A motor fault may not only cause economic loss but also casualties. Furthermore, during the past few decades, the focus of fault diagnosis research on induction motor was to explore how to efficiently monitor the induction motor to avoid motor failure.

Many methods have been put forward for fault diagnosis. An adaptive observer has been proposed in [21] to detect system faults. A fast adaptive fault estimation algorithm was proposed in ([22–24]) to enhance the accuracy of fault estimation. In this process, the estimators consist of proportional and integral items. Vector augmentation was performed using the robust observer to estimate the fault [25]. A sliding mode observer was applied to a high-speed train in [26], where linear matrix inequalities (LMIs) are used to ensure the robustness with respect to the interference. An unknown input observer (UIO) was proposed in [27], which eliminated the unknown input item. Methods for nonlinear system observers have been proposed, such as Lyapunov method, coordinate transformation method[28], extended Kalman filter, interval observer (IO) and feedback linearisation technology.

Recently, the interval observer approach has been extensively investigated, and some important achievements have been obtained. In [29], a class of interval observer was successfully designed for nonlinear systems, and the state of the error system could be guaranteed to be non-negative when the condition of the Metzler matrix was satisfied. In [30] and [31], the designed method of interval observer was studied for continuous and discrete linear time-invariant systems with bounded disturbances, based on the Jordan canonical form, and the appropriate of linear time-varying transformation. In [32], the designed method of interval observer was studied based on the Sylvester equation and the linear time-invariant transformation. In [29], the system control strategy based on an interval observer was studied.

In this paper, a fault estimation observer is proposed for high-speed railway traction devices with sensor fault and disturbances. The main contributions of this study are as follows. Firstly, an interval observer is designed based on the unknown input observer (UIO), which eliminates the effects of the external

disturbance on the fault diagnosis, and only uses partial information of the measurement output interval to ensure the real-time tracking of the original system. This process is different from the classical observer design, because the error system is asymptotically convergent to zero in the proposed design. Secondly, the observer is designed for the augmented system composed of a state vector and a fault. Then, a method for constructing the Metzler matrix for systems which do not satisfy the condition of the Metzler matrix is proposed. This technique is successfully applied to high-speed train motor system based on the observable standard form. Thirdly, the system parameter are found to enhance fault estimation performance.

The remainder of this paper is organised as follows: Preliminaries and problem formulation are presented in Section 2. Section 3 contains the design of interval observer and unknown input observer (IO-UIO)-based FD for the high-speed train and the coordinate transformation. Simulation results are provided to illustrate the effectiveness of the proposed methods in Section 4. Finally, a conclusion is made in Section 5.

2. Preliminaries and Problem Formulation

2.1. Preliminaries

$\mathbb{R}$ denotes a set of real numbers. $\mathbb{R} \geq 0$ denotes a set of non-negative real numbers, i.e., $\mathbb{R} \geq 0 := [0, \infty)$. I denotes the identity matrix in $\mathbb{R}^{n\times n}$. For vectors $x_a = [x_{a,1}, ..., x_{a,n}]^{\intercal} \in \mathbb{R}^n$ and $x_b = [x_{b,1}, ..., x_{b,n}]^{\intercal} \in \mathbb{R}^n$, the inequality $x_a \leq x_b$, if and only if $x_{a,i} \leq x_{b,i}$, for all $i = 1, ..., n$. For matrices $A = (a_{i,j})_{m\times n} \in \mathbb{R}^{m\times n}$ and $B = (b_{i,j})_{m\times n} \in \mathbb{R}^{m\times n}$, the inequality $A \geqslant B (A > B)$ denotes that $a_{i,j} \geqslant b_{i,j} (a_{i,j} > b_{i,j})$, $i = 1, ..., n$, $j = 1, ..., m$. For a square matrix $Q \in \mathbb{R}^{n\times n}$, let the matrix $Q^+ \in \mathbb{R}^{n\times n}$ denote $Q^+ = \max\{q_{i,j}, 0\})_{i,j=1,1}^{n,n}$ and $Q^- = Q^+ - Q$. The superscripts $+$ and $-$ are defined appropriately for other cases when they appear in the following sections.

The following definitions are given: a matrix $A \in \mathbb{R}^{n\times n}$ is called Hurwitz if all its eigenvalues have a negative real part, and it is called Metzler if all its

off-diagonal elements are non-negative.

The following lemmas will be used in the sequel.

Lemma 1[34]. The eigenvalues of a given matrix $\mathcal{A} \in \mathbb{R}^{n\times n}$ belong to the disk region $\mathcal{D}(\alpha,\tau)$ with centre $\alpha+j0$ and radius τ if and only if a symmetric positive definite matrix $\mathcal{P} \in \mathbb{R}^{n\times n}$ exists such that the following condition holds:

$$\begin{bmatrix} -\mathcal{P} & \mathcal{P}(\mathcal{A}-\alpha I_n) \\ * & -\tau^2\mathcal{P} \end{bmatrix} < 0 \tag{1}$$

Lemma 2[30]. Consider a vector variable $x \in \mathbb{R}^n$ satisfying $\underline{x} \leqslant x \leqslant \overline{x}$ with $\underline{x}, \overline{x} \in \mathbb{R}^n$, and a constant matrix $A \in \mathbb{R}^{m\times n}$, the following condition holds:

$$A^+\underline{x} - A^-\overline{x} \leqslant Ax \leqslant A^+\overline{x} - A^-\underline{x} \tag{2}$$

2.2. Problem Formulation

Consider the ideal mathematical model of the traction motor in the $d-q$ axis synchronous rotating reference frame [33] as follows:

$$\begin{cases} \dot{x}(t) = Ax(t) + Bu(t) + f_a(x(t)) \\ y(t) = Cx(t) \end{cases} \tag{3}$$

where

$$x(t) = \begin{bmatrix} x_1 & x_2 & x_3 & x_4 & x_5 \end{bmatrix}^{\mathrm{T}} = \begin{bmatrix} i_{qs} & i_{ds} & \lambda_{qr} & \lambda_{dr} & \omega_m \end{bmatrix}^{\mathrm{T}} \in \mathbb{R}^5,$$

is the state variable, $u(t) \in \mathbb{R}^2$ is the input variable and $y(t) \in \mathbb{R}^3$ is the output variable. A is the matrix of asynchronous motor system, whilst B is the input

distribution matrix of the system which are as follows:

$$A=\begin{bmatrix} -\gamma & -\omega_s & \alpha\beta & 0 & 0 \\ \omega_s & -\gamma & 0 & \alpha\beta & 0 \\ \alpha L_m & 0 & -\alpha & -\omega_s & 0 \\ 0 & \alpha L_m & \omega_s & \alpha & 0 \\ 0 & 0 & 0 & 0 & 0 \end{bmatrix}, B=\begin{bmatrix} \frac{1}{\delta L_s} & 0 \\ 0 & \frac{1}{\delta L_s} \\ 0 & 0 \\ 0 & 0 \\ 0 & 0 \end{bmatrix},$$

C is the output distribution matrix, and $f_a\left(x\left(t\right)\right)$ is the nonlinear part of the system given as follows:

$$C=\begin{bmatrix} 1 & 0 & 0 & 0 & 0 \\ 0 & 1 & 0 & 0 & 0 \\ 0 & 0 & 0 & 0 & 1 \end{bmatrix}, f_a\left(x\left(t\right)\right)=\begin{bmatrix} -n_p\beta x_5 x_4 \\ n_p\beta x_5 x_3 \\ n_p\beta x_5 x_4 \\ -n_p\beta x_5 x_3 \\ \mu\left(x_4 x_1 - x_3 x_2\right) - \frac{1}{J}T_L \end{bmatrix},$$

where

$$\delta = 1-\frac{L_m^2}{L_s L_r}, \alpha=\frac{R_r}{L_r}, \beta=\frac{L_m}{\delta L_s L_r},$$

$$\mu=\frac{3}{2}n_p\frac{L_m}{JL_r}, \gamma=\frac{L_m^2 R_r}{\delta L_s L_r^2}+\frac{R_s}{\delta L_s},$$

i_{qs} and i_{ds} denote the stator currents in the $d-q$ frame; λ_{qr} and λ_{dr} denote the rotor flues in the dq-frame; ω_m is the mechanical angular speed; ω_s is the synchronous rotating speed; L_s, L_r and L_m denote stator self inductance, rotor self inductance and state-rotor mutual inductance, respectively; T_L is the load torque; n_p is the pole pair number; and J is the moment inertia.

The CRH5 a adopts three-phase squirrel-cage asynchronous motor named 6FJA3257A, the parameters of which are shown in Table 1. The actual mathematical model of the traction motor can be represented as follows:

$$\begin{cases} \dot{x}\left(t\right)=Ax\left(t\right)+Bu\left(t\right)+f_a\left(x\left(t\right)\right)+E_d d\left(t\right) \\ y\left(t\right)=Cx\left(t\right)+E_f f\left(t\right) \end{cases} \tag{4}$$

where $d(t) \in \mathbb{R}^1$ is the disturbance vector, and $f(t) \in \mathbb{R}^1$ represents the sensor fault. E_d and E_f are the disturbance distribution matrix, and fault distribution matrix, respectively. A, B, E_f, C and E_d are constant real matrices of appropriate dimensions. In addition, matrices E_f and E_d are of full column rank given as follows:

$$E_f = \begin{bmatrix} 1 \\ 0 \\ 0 \end{bmatrix}, E_d = \begin{bmatrix} 0 & 0 & 0 & 0 & -\frac{1}{J} \end{bmatrix}^{\mathrm{T}},\ d(t) = \Delta T_L.$$

The following table records the relevant parameters of the asynchronous motor:

Table 1: Asynchronous motor 6FJA3257A

no	parameter	value
1	Stator resistance R_s	105.1 $m\Omega$
2	Stator inductance L_s	31.7 mH
3	Rotor resistance R_r	91.9 $m\Omega$
4	Rotor inductance L_r	31.7 mH
5	Mutual inductance L_m	29.9 mH
6	The moment inertia J	15 $kg \cdot m^2$
7	The load torque T_L	4500 $N \cdot m$
8	The pole pairs number n_p	3
9	The Motor rotation speed w_s	$2 * pi * 60$ rad/s

Remark 1. Available results of the interval observer for the induction motor are very few. This paper mainly focuses on how to estimate the fault of a system with the nonlinear part of CRH5 and how to improve the performance of fault estimation. An IO-UIO is designed to eliminate the effect of load torque disturbance on the fault estimation.

3. Main Results

3.1. IO-UIO Based Fault Estimation Design

In this subsection, an observer is designed to estimate the incipient sensor faults. Interval information is applied to deal with the nonlinear part of the

system. The augmented fault estimator is introduced, and the sensor fault vector is considered as the auxiliary state vector.

The original system (4) can be rewritten in the following form:

$$\begin{cases} \begin{bmatrix} \dot{x}(t) \\ \dot{f}(t) \end{bmatrix} = \begin{bmatrix} A & 0 \\ 0 & 0 \end{bmatrix} \begin{bmatrix} x(t) \\ f(t) \end{bmatrix} + \begin{bmatrix} B \\ 0 \end{bmatrix} u(t) + \begin{bmatrix} E_d \\ 0 \end{bmatrix} d(t) \\ \qquad\qquad + \begin{bmatrix} f_a\left(x\left(t\right)\right) \\ 0 \end{bmatrix} + \begin{bmatrix} 0 \\ I_r \end{bmatrix} \dot{f}(t) \\ y(t) = \begin{bmatrix} C & E_f \end{bmatrix} \begin{bmatrix} x(t) \\ f(t) \end{bmatrix} \end{cases} \tag{5}$$

For convenience, the following parameters are defined: augmented state vector $\overline{x}(t) = \begin{bmatrix} x(t) \\ f(t) \end{bmatrix}$, augmented state distribution matrix $\bar{A} = \begin{bmatrix} A & 0 \\ 0 & 0 \end{bmatrix}$, augmented input distribution matrix $\bar{B} = \begin{bmatrix} B \\ 0 \end{bmatrix}$, augmented output distribution matrix $\bar{C} = \begin{bmatrix} C & E_f \end{bmatrix}$, augmented nonlinear vector $\bar{f}_a\left(x\left(t\right)\right) = \begin{bmatrix} f_a\left(x\left(t\right)\right) \\ 0 \end{bmatrix}$, augmented disturbance distribution matrix $\bar{E}_d = \begin{bmatrix} E_d \\ 0 \end{bmatrix}$, and augmented Fault distribution matrix $\bar{I}_r = \begin{bmatrix} 0 \\ I_r \end{bmatrix}$.

Then, system(5) can be rewritten as follows:

$$\begin{cases} \dot{\bar{x}}(t) = \bar{A}\bar{x}(t) + \bar{B}u(t) + \bar{E}_d d(t) + \bar{f}_a\left(x\left(t\right)\right) + \bar{I}_r \dot{f}(t) \\ y(t) = \bar{C}\,\bar{x}(t) \end{cases} \tag{6}$$

where $\dot{f}(t)$ is the derivative of the fault $f(t)$, and I_r is an $r \times r$-dimensional unit matrix.

Combining with $\bar{T} + \bar{H}\bar{C} = I$, an equivalent augmented system state space

description form can be obtained as follows:

$$\begin{cases} \dot{\bar{x}}(t) = \bar{A}\bar{x}(t) + \bar{B}u(t) + \bar{E}_d d(t) + \bar{I}_r \dot{f}(t) + \bar{f}_a\left(x\left(t\right)\right) + \bar{H}\dot{y}(t) - \bar{H}\bar{C}\dot{\bar{x}}(t) \\ \quad = \bar{A}\bar{x}(t) + \bar{B}u(t) + \bar{E}_d d(t) + \bar{I}_r \dot{f}(t) + \bar{H}\dot{y}(t) - \ \bar{H}\bar{C}(\bar{A}\bar{x}(t) + \bar{B}u(t) \\ \quad\quad + \bar{E}_d d(t) + \ \bar{I}_r \dot{f}(t) + \bar{f}_a\left(x\left(t\right)\right)) \\ \quad = \bar{T}\bar{A}\bar{x}(t) + \bar{T}\bar{B}u(t) + \bar{T}\bar{E}_d d(t) + \bar{T}\bar{f}_a\left(x\left(t\right)\right) + \ \bar{T}\bar{I}_r \dot{f}(t) + \bar{H}\dot{y}(t) \\ y(t) = \bar{C}\,\bar{x}(t) \end{cases} \tag{7}$$

where$\bar{H}$ and $\bar{T}$ are the design parameters with appropriate dimensions.

Assumption 1. The pair $(\bar{T}\bar{A}, \bar{C})$ is observable and $\text{rank}(\bar{C}\bar{E}_d) = \text{rank}(\bar{E}_d)$.

Lemma 3[36]. Under Assumption 1, the expression described by (8) is a UIO for system (7).

For system (9), the problem of fault estimation is converted to IO-UIO design to reconstruct the fault vector. An observer is proposed to achieve fault estimation as follows:

$$\begin{cases} \dot{\bar{z}}(t) = \bar{T}\bar{A}\hat{\bar{x}}(t) + \bar{T}\bar{B}u(t) + \bar{T}\bar{f}_a\left(x\left(t\right)\right) - \bar{L}\left(\hat{y}(t) - y(t)\right) \\ \hat{\bar{x}}(t) = \bar{z}(t) + \bar{H}y(t) \\ \hat{f}(t) = \bar{I}_r^T \hat{\bar{x}}(t) \\ \hat{y}(t) = \bar{C}\hat{\bar{x}}(t) \end{cases} \tag{8}$$

where $\bar{T} + \bar{H}\bar{C} = I$. $\bar{z}(t)$ is an unknown input augmented variable, whilst $\hat{\bar{x}}(t)$ and $\hat{\bar{y}}(t)$ denote the augmented state vector and output vector. $\hat{f}(t)$ is the sensor fault estimate value, whilst matrices $\bar{H}$, $\bar{T}$ and $\bar{L}$ are the gain matrices of the unknown input observer.

Assumption 2. Given that the arbitrary $\bar{x}^-\left(t\right) \leqslant \bar{x}\left(t\right) \leqslant \bar{x}^+\left(t\right)$, vector functions $\bar{f}_a^-\left(x^+\left(t\right), x^-\left(t\right)\right)$ and $\bar{f}_a^+\left(x^+\left(t\right), x^-\left(t\right)\right)$ exist and satisfy the following:

$$\bar{f}_a^-\left(x^+\left(t\right), x^-\left(t\right)\right) \leqslant \bar{f}_a\left(x\left(t\right)\right) \leqslant \bar{f}_a^+\left(x^+\left(t\right), x^-\left(t\right)\right)$$

where $\bar{x}^-\left(t\right)$ and $\bar{x}^+\left(t\right)$ denote the lower and upper bounds of the augmented

state vector, respectively.

Assumption 3. Matrix $\bar{L}$ exists such that the matrix $(\bar{T}\bar{A} - \bar{L}\bar{C})$ is Metzler.

The interval observer is designed based on an unknown input observer. Under Assumption 2, the IO-UIO is described as follows:

The upper bound observer is as follows:

$$\begin{cases} \dot{\hat{z}}^{+}(t) = \bar{T}\bar{A}\hat{\bar{x}}^{+}(t) + \bar{T}\bar{B}u(t) + \bar{T}\bar{f}_a^{+}\left(x\left(t\right)\right) - \bar{L}\left(\hat{y}^{+}(t) - y(t)\right) \\ \hat{\bar{x}}^{+}(t) = \bar{z}^{+}(t) + \bar{H}y^{+}(t) \\ \hat{f}^{+}(t) = \bar{I}_r^{T}\hat{\bar{x}}^{+}(t) \\ \hat{y}^{+}(t) = \bar{C}\hat{\bar{x}}^{+}(t) \end{cases} \tag{9}$$

The lower bound observer is as follows:

$$\begin{cases} \dot{\hat{z}}^{-}(t) = \bar{T}\bar{A}\hat{\bar{x}}^{-}(t) + \bar{T}\bar{B}u(t) + \bar{T}\bar{f}_a^{-}\left(x\left(t\right)\right) - \bar{L}\left(\hat{y}^{-}(t) - y(t)\right) \\ \hat{\bar{x}}^{-}(t) = \bar{z}^{-}(t) + \bar{H}y^{-}(t) \\ \hat{f}^{-}(t) = \bar{I}_r^{T}\hat{\bar{x}}^{-}(t) \\ \hat{y}^{-}(t) = \bar{C}\hat{\bar{x}}^{-}(t) \end{cases} \tag{10}$$

where $\bar{z}^{+}(t)$ and $\bar{z}^{-}(t)$ represent the state of the upper and lower bounds of the observers, respectively, and $\bar{T} + \bar{H}\bar{C} = I$.

Theorem 1. Under Assumptions 2 and 3, if the initial conditions are satisfied, and the constraint $x^{-}(0) \leqslant x(0) \leqslant x^{+}(0)$, then the solutions of systems (7), (9) and (10) satisfy the following:

$$\hat{\bar{x}}^{-}(t) \leqslant \bar{x}(t) \leqslant \hat{\bar{x}}^{+}(t),\ \forall t \geqslant 0.$$

Proof: The augmented system error dynamic equation is considered. For the upper bound observer, let $\bar{e}_x^{+}(t) = \hat{\bar{x}}^{+}(t) - \bar{x}(t)$, ${e_y}^{+}(t) = \hat{y}^{+}(t) - y(t) = \bar{C}\bar{e}_x^{+}(t)$, and ${e_f}^{+}(t) = \hat{f}^{+}(t) - f(t)$.

Then, from (6) and (7), the system's error state equation is expressed as

follows:

$$\begin{aligned}\dot{\bar{e}}_x^+(t) &= \dot{\hat{\bar{x}}}^+(t) - \dot{\bar{x}}(t) = \bar{T}\bar{A}\hat{\bar{x}}^+(t) + \bar{T}\bar{B}u(t) - \bar{L}\left(\hat{y}^+(t) - y(t)\right) \\ &\quad + \bar{T}\bar{f}_a^+\left(x\left(t\right)\right) + \bar{H}\dot{y}(t) - \bar{T}\bar{A}\bar{x}^+(t) - \bar{T}\bar{B}u(t) - \bar{T}\bar{E}_d d(t) \\ &\quad - \bar{T}\bar{I}_r\dot{f}(t) - \bar{T}\bar{f}_a\left(x\left(t\right)\right) - \bar{H}\dot{y}(t) \\ &= \bar{T}\bar{A}\bar{e}_x^+(t) - \bar{L}\left(\hat{y}^+(t) - y(t)\right) - \bar{T}\bar{E}_d d(t) - \bar{T}\bar{I}_r\dot{f}(t) \\ &\quad + \bar{T}\left(\bar{f}_a^+\left(x\left(t\right)\right) - \bar{f}_a\left(x\left(t\right)\right)\right) \\ &= \left(\bar{T}\bar{A} - \bar{L}\bar{C}\right)\bar{e}_x^+(t) - \bar{T}\bar{E}_d d(t) - \bar{T}\bar{I}_r\dot{f}(t) \\ &\quad + \bar{T}\bar{f}_a^+\left(x\left(t\right)\right) - \bar{T}\bar{f}_a\left(x\left(t\right)\right)\end{aligned} \tag{11}$$

When the following conditions are satisfied, the disturbance can be completely eliminated,

$$\bar{T}\bar{E}_d = 0$$

where $\bar{E}_d$ and $\bar{C}$ are known. Thus, the unknown matrix $\bar{H}$ can be obtained according to $\bar{T}\bar{E}_d = 0$ and $\bar{T} + \bar{H}\bar{C} = I$.

The simplified error dynamic system can be obtained from (11) as follows:

$$\begin{cases}\dot{\bar{e}}_x^+(t) = \left(\bar{T}\bar{A} - \bar{L}\bar{C}\right)\bar{e}_x^+(t) + \bar{T}\left(\bar{f}_a^+\left(x\left(t\right)\right) - \bar{f}_a\left(x\left(t\right)\right)\right) - \bar{T}\bar{I}_r\dot{f}(t). \\ {e_f}^+(t) = \bar{I}_r^T\bar{e}_x^+(t)\end{cases} \tag{12}$$

Similarly, for the lower bound observer, by denoting system the augmented state error $\bar{e}_x^-(t) = \bar{x}(t) - \hat{\bar{x}}^-(t)$, augmented output estimation error ${e_y}^-(t) = y(t) - \hat{y}^-(t) = \bar{C}\bar{e}_x^-(t)$, and the error of lower bound of fault and true value is ${e_f}^-(t) = f(t) - \hat{f}^-(t)$. Then, the system's error state equation is expressed as follows:

$$\begin{cases}\dot{\bar{e}}_x^-(t) = \left(\bar{T}\bar{A} - \bar{L}\bar{C}\right)\bar{e}_x^-(t) + \bar{T}\left(\bar{f}_a\left(x\left(t\right)\right) - \bar{f}_a^-\left(x\left(t\right)\right)\right) + \bar{T}\bar{I}_r\dot{f}(t). \\ {e_f}^-(t) = \bar{I}_r^T\bar{e}_x^-(t)\end{cases} \tag{13}$$

By assumption 2, we have $\bar{e}_x^+(0) > 0$, $\bar{e}_x^-(0) > 0$. From assumption 3, the dynamics of the estimation errors are cooperative. Therefore, $\bar{e}_x^+(t) > 0$, $\bar{e}_x^-(t) > 0$

for all $t \geqslant 0$. □

Remark 2. Compared with the Luenberger Observer, the observer we studied can eliminate the impact of external disturbances on fault estimation when the hypothetical condition $\bar{T}\bar{E}_d = 0$ is satisfied. Consequently, this method effectively simplifies the algorithm and improves the performance of fault estimation. In dealing with the nonlinear part of the system, the method proposed in this paper involves the designing of an interval observer using part of the measurement information to replace a single point of measurement with a reasonable interval.

Theorem 2. The observer gain matrix $\bar{L}$ of the fault estimation for high-speed train can be obtained by solving the following linear matrix inequality (LMI), and the H_∞ performance level γ and a circular region $\mathcal{D}(\alpha, \tau)$ are provided. If a symmetric positive definite matrix $\bar{Q} \in \mathbb{R}^{(n+r)\times(n+r)}$ and matrix $\bar{L} \in \mathrm{R}^{(n+r)\times p}$, $\bar{Y} \in \mathrm{R}^{(n+r)\times p}$ satisfies the following:

$$\begin{bmatrix} -\bar{Q} & \bar{Q}\bar{T}\bar{A} - \bar{Y}\bar{C} - \alpha\bar{Q} \\ * & -\tau^2\bar{Q} \end{bmatrix} < 0 \tag{14}$$

$$\begin{bmatrix} \varphi & -\bar{Q}\bar{T}\bar{I}_r & \bar{I}_r \\ * & -\gamma I & 0 \\ * & * & -\gamma I \end{bmatrix} < 0 \tag{15}$$

where $\varphi = \bar{Q}\bar{T}\bar{A} + \left(\bar{T}\bar{A}\right)^{\mathrm{T}}\bar{Q} - \bar{Y}\bar{C} - \left(\bar{Y}\bar{C}\right)^{\mathrm{T}}$, and the eigenvalues of $(\bar{T}\bar{A} - \bar{L}\bar{C})$ belong to $\mathcal{D}(\alpha, \tau)$.

Proof: Constraint (14): Substituting $(\bar{T}\bar{A} - \bar{L}\bar{C})$ into $\mathcal{A}$ and $\bar{P}$ into $\mathcal{P}$ in Lemma 1, we can obtain (14).

Constraint (15): Consider the following Lyapunov function:

$$V(t) = \bar{e}_x(t)\bar{P}\bar{e}_x(t) \tag{16}$$

Its derivative with respect to time is

$$\dot{V}(t) = \bar{e}_x^{\intercal}(t)(\bar{Q}(\bar{T}\bar{A} - \bar{L}\bar{C}) + (\bar{T}\bar{A} - \bar{L}\bar{C})^{\intercal}\bar{Q})\bar{e}_x - 2\bar{e}_x^{\intercal}(t)\bar{Q}\bar{T}\bar{I}_r\dot{f}(t) \tag{17}$$

Let us define:

$$J_1 = \int_{t_f}^{\infty} \frac{1}{\gamma} e_f^{\intercal}(t)e_f(t) - \gamma \dot{f}^{\intercal}(t)\dot{f}(t)d(t) \tag{18}$$

one can obtain:

$$\begin{aligned} J_1 &\leqslant \int_{t_f}^{\infty} \dot{V}(t) + \frac{1}{\gamma} e_f^{\intercal}(t)e_f(t) - \gamma \dot{f}^{\intercal}(t)\dot{f}(t)d(t) \\ &= \int_{t_f}^{\infty} \dot{V}(t) + \frac{1}{\gamma} \bar{e}_x^{\intercal}(t)\bar{I}_r\bar{I}_r^{\intercal}\bar{e}_x(t) - \gamma \dot{f}^{\intercal}(t)\dot{f}(t)d(t) \end{aligned} \tag{19}$$

From (17), it follows that:

$$\begin{aligned} &\dot{V}(t) + \frac{1}{\gamma} \bar{e}_x^{\intercal}(t)\bar{I}_r\bar{I}_r^{\intercal}\bar{e}_x(t) - \gamma \dot{f}^{\intercal}(t)\dot{f}(t) \\ &= \bar{e}_x^{\intercal}(t)(\bar{Q}(\bar{T}\bar{A} - \bar{L}\bar{C}) + (\bar{T}\bar{A} - \bar{L}\bar{C})^{\intercal}\bar{Q})\bar{e}_x(t) \\ &\quad - 2\bar{e}_x^{\intercal}(t)\bar{Q}\bar{T}\bar{I}_r\dot{f}(t) + \frac{1}{\gamma} \bar{e}_x^{\intercal}(t)\bar{I}_r\bar{I}_r^{\intercal}\bar{e}_x(t) \quad - \gamma \dot{f}^{T}(t)\dot{f}(t) \\ &= \zeta^{T}(t)\Xi\zeta(t) \end{aligned} \tag{20}$$

where

$$\zeta(t) = \begin{bmatrix} \bar{e}_x(t) \\ \dot{f}(t) \end{bmatrix},$$

$$\Xi = \begin{bmatrix} \bar{Q}(\bar{T}\bar{A} - \bar{L}\bar{C}) + (\bar{T}\bar{A} - \bar{L}\bar{C})^{\intercal}\bar{Q} + \frac{1}{\gamma}\bar{I}_r\bar{I}_r^{T} & * \\ -\bar{Q}\bar{T}\bar{I}_r & -\gamma I \end{bmatrix}^{\intercal}$$

Through the Schuur complement, $\Xi < 0$ becomes

$$\begin{bmatrix} \bar{Q}(\bar{T}\bar{A} - \bar{L}\bar{C}) + (\bar{T}\bar{A} - \bar{L}\bar{C})^{\intercal}\bar{Q} & -\bar{Q}\bar{T}\bar{I}_r & \bar{I}_r \\ * & -\gamma I & 0 \\ * & * & -\gamma I \end{bmatrix} < 0 \tag{21}$$

which is equal to (15). Thus, (12) and (13) are stable and satisfy the H_∞

performance $||e_f(t)||_2 < \gamma||\dot{f}(t)||_2$ if condition (15) holds. □

Remark 3. The observer gain matrix is given by $\bar{L} = \bar{Q}^{-1}\bar{Y}$. The algorithm which satisfies the robust H_∞ performance index can effectively restrain the influence of fault derivative $\dot{f}(t)$ on fault estimation error $e_f(t)$.

3.2. Transformation of Coordinates

However, the corresponding observer gain matrix $\bar{L}$ cannot be determined. This value can make $(\bar{T}\bar{A} - \bar{L}\bar{C})$ be a Metzler matrix from the nonlinear system of the investigated traction motor for high-speed trains. A non-singular constant transformation matrix is given to solve the problem, and a new system equation is obtained by equivalent transformation $\bar{\xi}(t) = P\bar{x}(t)$.

$$\begin{cases} \dot{\bar{\xi}}(t) = P\bar{A}P^{-1}\bar{\xi}(t) + P\bar{B}u(t) + P\bar{E}_d d(t) + P\bar{f}_a(x(t)) + P\bar{I}_r\dot{f}(t) \\ y(t) = \bar{C}P^{-1}\bar{\xi}(t) \end{cases} \tag{22}$$

An equivalent augmented system state space description form can be obtained as follows:

$$\begin{cases} \dot{\bar{\xi}}(t) = P\bar{T}\bar{A}P^{-1}\bar{\xi}(t) + P\bar{T}\bar{B}u(t) + P\bar{T}\bar{E}_d d(t) + P\bar{T}\bar{f}_a(x(t)) \\ \qquad\qquad + P\bar{T}\bar{I}_r\dot{f}(t) + P\bar{H}\dot{y}(t) \\ y(t) = \bar{C}P^{-1}\bar{\xi}(t) \end{cases} \tag{23}$$

When $\bar{T}\bar{E}_d = 0$ is considered, the simplified form can be obtained from (23) as follows:

$$\begin{cases} \dot{\bar{\xi}}(t) = P\bar{T}\bar{A}P^{-1}\bar{\xi}(t) + P\bar{T}\bar{B}u(t) + P\bar{T}\bar{f}_a(x(t)) + P\bar{T}\bar{I}_r\dot{f}(t) + P\bar{H}\dot{y}(t) \\ y(t) = \bar{C}P^{-1}\bar{\xi}(t) \end{cases} \tag{24}$$

The interval observer is constructed as follows:

$$\begin{cases} \dot{\hat{\bar{\xi}}}^{+}(t) = P\bar{T}\bar{A}P^{-1}\hat{\bar{\xi}}^{+}(t) + P\bar{T}\bar{B}u(t) - P\bar{L}(\bar{C}P^{-1}\hat{\bar{\xi}}^{+}(t) - y(t) \\ \qquad\qquad + P\bar{T}\bar{f}_a^{+}\left(x\left(t\right)\right) + P\bar{H}\dot{y}(t) \\ \qquad\quad = R\hat{\bar{\xi}}^{+}(t) + P\bar{T}\bar{B}u(t) + P\bar{T}\bar{f}_a^{+}\left(x\left(t\right)\right) + P\bar{H}\dot{y}(t) + P\bar{L}y(t) \\ \dot{\hat{\bar{\xi}}}^{-}(t) = P\bar{T}\bar{A}P^{-1}\hat{\bar{\xi}}^{-}(t) + P\bar{T}\bar{B}u(t) - P\bar{L}(\bar{C}P^{-1}\hat{\bar{\xi}}^{-}(t) - y(t) \\ \qquad\qquad + P\bar{T}\bar{f}_a^{-}\left(x\left(t\right)\right) + P\bar{H}\dot{y}(t) \\ \qquad\quad = R\hat{\bar{\xi}}^{-}(t) + P\bar{T}\bar{B}u(t) + P\bar{T}\bar{f}_a^{-}\left(x\left(t\right)\right) + P\bar{H}\dot{y}(t) + P\bar{L}y(t) \end{cases} \tag{25}$$

where R is equal to $P(\bar{T}\bar{A} - \bar{L}\bar{C})P^{-1}$ and $\hat{\bar{\xi}}^{+}(t)$, $\hat{\bar{\xi}}^{-}(t)$ denote the upper and lower bounds of the augmented observer vector after the transformation of coordinates. Moreover, $\bar{f}_a^{\bar{\xi}}\left(x\left(t\right)\right)$ denotes the nonlinear part after the coordinates have been transformed.

The following variables are defined:

$$\begin{aligned} \bar{\varphi}^{+}\left(\bar{\xi}^{-}\left(\mathrm{t}\right),\bar{\xi}^{+}\left(\mathrm{t}\right)\right) &= \bar{f}_a^{+}\left(\bar{P}_i\bar{\xi}^{-}\left(\mathrm{t}\right) - \underline{\mathrm{P}}_i\bar{\xi}^{+}\left(\mathrm{t}\right), \bar{P}_i\bar{\xi}^{+}\left(\mathrm{t}\right) - \underline{\mathrm{P}}_i\bar{\xi}^{-}\left(\mathrm{t}\right)\right) \\ \bar{\varphi}^{-}\left(\bar{\xi}^{-}\left(\mathrm{t}\right),\bar{\xi}^{+}\left(\mathrm{t}\right)\right) &= \bar{f}_a^{-}\left(\bar{P}_i\bar{\xi}^{-}\left(\mathrm{t}\right) - \underline{\mathrm{P}}_i\bar{\xi}^{+}\left(\mathrm{t}\right), \bar{P}_i\bar{\xi}^{+}\left(\mathrm{t}\right) - \underline{\mathrm{P}}_i\bar{\xi}^{-}\left(\mathrm{t}\right)\right) \end{aligned}$$

where $\bar{\xi}^{+} and\ \bar{\xi}^{-}$ represent the upper and lower bounds of the augmented state vector after the coordinates have been transformed.

Under Assumption 2, the following can be obtained:

$$\begin{aligned} \bar{f}_a^{\bar{\xi}-}\left(\bar{\xi}^{-}\left(t\right),\bar{\xi}^{+}\left(t\right)\right) &= \bar{P}\bar{\varphi}^{-}\left(\bar{\xi}^{-}\left(t\right),\bar{\xi}^{+}\left(t\right)\right) - \underline{\mathrm{P}}\bar{\varphi}^{+}\left(\bar{\xi}^{-}\left(t\right),\bar{\xi}^{+}\left(t\right)\right) \\ &\leqslant P\bar{f}_a\left(P^{-1}\bar{\xi}\left(t\right)\right) \\ &\leqslant \bar{P}\bar{\varphi}^{+}\left(\bar{\xi}^{-}\left(t\right),\bar{\xi}^{+}\left(t\right)\right) - \underline{\mathrm{P}}\bar{\varphi}^{-}\left(\bar{\xi}^{-}\left(t\right),\bar{\xi}^{+}\left(t\right)\right) \\ &= \bar{f}_a^{\bar{\xi}+}\left(\bar{\xi}^{-}\left(t\right),\bar{\xi}^{+}\left(t\right)\right). \end{aligned} \tag{26}$$

where $\bar{P} = \max\{0, P\}$, $\underline{\mathrm{P}} = \bar{P} - P$, $\bar{P}_i = \max\left\{0, P^{-1}\right\}$ and $\underline{\mathrm{P}}_i = \bar{P}_i - P^{-1}$.

The upper bound error $\bar{e}^{\bar{\xi}+}\left(t\right)$ and lower bound error $\bar{e}^{\bar{\xi}-}\left(t\right)$ are defined as

follows:

$$\bar{e}^{\bar{\xi}+}(t) = \hat{\bar{\xi}}^{+}(t) - \bar{\xi}(t)$$
$$\bar{e}^{\bar{\xi}-}(t) = \bar{\xi}(t) - \hat{\bar{\xi}}^{-}(t)$$

Then, the error dynamic equation can be obtained as follows:

$$\begin{cases} \dot{\bar{e}}^{\bar{\xi}+}(t) = R\bar{e}^{\bar{\xi}+}(t) + P\left[\bar{f}_a^{+}(x(t)) - \bar{f}_a(x(t))\right] - P\bar{T}\bar{I}_r\dot{f}(t) \\ \dot{\bar{e}}^{\bar{\xi}-}(t) = R\bar{e}^{\bar{\xi}-}(t) + P\left[\bar{f}_a(x(t)) - \bar{f}_a^{-}(x(t))\right] - P\bar{T}\bar{I}_r\dot{f}(t) \end{cases} \tag{27}$$

Theorem 3. Let the matrix $(\bar{T}\bar{A} - \bar{L}\bar{C})$ and a Metzler matrix R have the same eigenvalues for some $\bar{L}$. If two vectors $\bar{e}_1$ and $\bar{e}_2$ exist such that the pairs $(\bar{T}\bar{A} - \bar{L}\bar{C},\ \bar{e}_1)$ and $(R,\ \bar{e}_2)$ are observable, then

$$P = O_2^{-1}O_1.$$

satisfies Sylvester equation: $P\bar{T}\bar{A} - RP = N\bar{C}$, $N = P\bar{L}$.

where

$$O_1 = \begin{bmatrix} \bar{e}_1 \\ \vdots \\ \bar{e}_1\big(\bar{T}\bar{A} - \bar{L}\bar{C}\big)^{n-1} \end{bmatrix},\ O_2 = \begin{bmatrix} \bar{e}_2 \\ \vdots \\ \bar{e}_2 R^{n-1} \end{bmatrix}.$$

Proof: Since the pairs $(\bar{T}\bar{A} - \bar{L}\bar{C},\ \bar{e}_1)$ and $(R,\ \bar{e}_2)$ are observable, matrices O_1 and O_2 are nonsingular. The following equation can be obtained through the transformation:

$$O_1(\bar{T}\bar{A} - \bar{L}\bar{C})O_1^{-1} = O_2 R O_2^{-1}$$

where $O_1(\bar{T}\bar{A} - \bar{L}\bar{C})O_1^{-1}$ and $O_2 R O_2^{-1}$ are canonical observability forms. The vectors $\bar{e}_1$ and $\bar{e}_2$ can be found if the pair $(\bar{T}\bar{A}, \bar{C})$ is observable. □

Remark 4. The Metzler matrices are constructed as follows: Let R be the lower triangular matrix, with the main diagonal elements as the eigenvalues of $(\bar{T}\bar{A} - \bar{L}\bar{C})$, and the elements below the main diagonal are positive. Moreover, the matrix R after transformation satisfies the property of Hurwitz and is a matrix Metzler at the same time. Combined with the above process, $\hat{\bar{\xi}}^{-}(t) \leqslant \bar{\xi}(t) \leqslant \hat{\bar{\xi}}^{+}(t),\ t \geqslant 0$. Then, the fault estimate is obtained by $\hat{f}^{+}(t) = \bar{I}_r^T\hat{\bar{x}}^{+}(t),\ \hat{f}^{-}(t) =$

$\bar{I}_r^T \hat{\bar{x}}^-(t)$.

3.3. Enhancement of the Accuracy of IO-UIO

When the interval observer is used to estimate the fault, the response time and the accuracy of the interval, that is, the difference between the upper and lower bounds of the interval observer, are considered. This subsection focuses on finding a performance index related to the interval accuracy based on the CRH5 motor system, which makes the interval size adjustable.

Since the equivalent transformation does not affect the experimental results, the system can be conveniently investigated based on the previous transformation before. The dynamic error equation can be derived from (12) and (13).

$$x(t) = \begin{bmatrix} x_1 & x_2 & x_3 & x_4 & x_5 & x_6 \end{bmatrix}^{\mathrm{T}} = \begin{bmatrix} i_{qs} & i_{ds} & \lambda_{qr} & \lambda_{dr} & \omega_m & f \end{bmatrix}^{\mathrm{T}}$$

Then, the following can be obtained:

$$\psi \dot{\bar{e}}_x = \psi(\bar{T}\bar{A} - \bar{L}\bar{C})\bar{e}_x + \psi\bar{T}(\bar{f}_a^+ - \bar{f}_a^-) \tag{28}$$

where $\psi = \begin{bmatrix} 0 & 0 & 0 & 0 & 0 & 1 \end{bmatrix}$.

Equation (22) can be simplified as follows:

$$\dot{e}_f = -l_{61}e_{x1} + l_{62}e_{x2} - l_{61}e_f \tag{29}$$

where l_{61} represents the first column of the sixth row of the observer gain matrix $\bar{L}$, and l_{62} represents the second column of the sixth row of this matrix. Moreover, the interval size of the fault estimate is related to the values of e_{x1}, e_{x2} and e_f. Moreover, the interval size can be regulated by l_{61} and l_{62}.

Remark 5. Equation (29) is not generic and is extracted from the characteristics of CRH5. Hence, this equation will no longer be applied in changing other systems or system parameters. However, the method is general, and a performance index can be found according to.

4. Simulation Results

In this section, numerical and simulation results are used to verify the feasibility of the proposed method for CRH5 (6FJA3257A). First part of this section discusses the fault estimation with regional pole placement. In the second part, we changed the numerical value of the performance index. Then, we compare the influence of the performance parameters on the fault estimation precision from the residual of the upper and lower bounds of the fault estimation curve in the simulation diagram.

According to the high-speed train traction motor system, the state vectors under stable operation can be obtained as follows:

$$x(t) = \begin{bmatrix} -150.3 & -222 & 0.3958 & -6.3345 & 124.9053 \end{bmatrix}^{\mathrm{T}}$$

Set the upper and lower bounds of the state vectors:

$$\begin{cases} x^{+}(t) = \begin{bmatrix} -150.0 & -221 & 0.40 & -6.32 & 125.5 \end{bmatrix}^{\mathrm{T}} \\ x^{-}(t) = \begin{bmatrix} -150.6 & -223 & 0.39 & -6.34 & 124.5 \end{bmatrix}^{\mathrm{T}} \end{cases}$$

it is obviously satisfying to assumption 2.

We illustrate the simulation results with the fault of q-axis stator current sensor.

The fault model is as follows:

$$f(t) = \begin{cases} 0\ , & 0s \leqslant t < 20s \\ 10, & t \geqslant 20s \end{cases}$$

Part 1. Fault estimation with regional pole placement.

We can solve (14) and (15) to obtain the observer gain matrix by choosing the region pole $\mathcal{D}(-20, 50)$.

Remark 6. When constraints (14) and (15) using the LMI toolbox of Matlab (2014b) are satisfied, the eigenvalues of $(\bar{T}\bar{A} - \bar{L}\bar{C})$ are located in the left half plane of the coordinate virtual axis and within the pole configuration circle.

The LMI region is as follows:

$$\mathrm{D} = \{\ \mathrm{z} \in \mathrm{C}\text{: Re(z)}\ < 0\}, \quad f_D(z) = z + \bar{z} < 0.$$

where $f_D(z)$ is the characteristic function of D. We choose $\mathcal{D}(-20, 50)$ to improve the performance of the system.

Parameters $\bar{Q}$, $\bar{Y}$ and $\bar{L}$ can be calculated as follows:

$$\bar{Q} = \begin{bmatrix} 0.5649 & 0.0193 & -0.0810 & -1.4510 & 0 & -0.2635 \\ 0.0193 & 0.0855 & 0.2357 & -0.0766 & 0 & 0.3055 \\ -0.0810 & 0.2357 & 0.7229 & 0.1294 & 0 & 0.8062 \\ -1.4510 & -0.0766 & 0.1294 & 3.7438 & 0 & 0.6428 \\ 0 & 0 & 0 & 0 & 2.0965 & 0 \\ -0.2635 & 0.3055 & 0.8062 & 0.6428 & 0 & 3.4594 \end{bmatrix}.$$

$$\bar{Y} = \begin{bmatrix} \text{- } 11.7195 & \text{- } 212.4609 & 0 \\ 28.1386 & \text{- } 9.4913 & 0 \\ 75.9143 & 23.3952 & 0 \\ 21.5699 & 545.5703 & 0 \\ 0 & 0 & 87.8535 \\ 129.4668 & 83.6815 & 0 \end{bmatrix}, \bar{L} = \begin{bmatrix} 21.6346 & \text{- } 669.2785 & 0 \\ 757.2506 & 23.6974 & 0 \\ -145.1688 & -28.8060 & 0 \\ 34.7317 & -111.9553 & 0 \\ 0 & 0 & 41.9045 \\ -0.4252 & -1.3582 & 0 \end{bmatrix}$$

Through $\bar{T} + \bar{H}\bar{C} = I$, H can be obtained when $\bar{T}$ and $\bar{C}$ are known.

$$\bar{H} = \begin{bmatrix} 0 & 0 & 0 \\ 0 & 0 & 0 \\ \text{- } 0.0031 & 0 & 0 \\ 0 & \text{- } 0.0031 & 0 \\ 0 & 0 & 1 \\ 0 & 0 & 0 \end{bmatrix}$$

From subsection A, matrix $\bar{T}$ can be calculated through $\bar{T}\bar{E}_d = 0$, because

$$\bar{E}_d = \begin{bmatrix} 0 & 0 & 0 & 0 & -1/15 & 0 \end{bmatrix}^{\mathrm{T}}$$

then,

$$\bar{T} = \begin{bmatrix} 1 & 0 & 0 & 0 & 0 & 0 \\ 0 & 1 & 0 & 0 & 0 & 0 \\ 0.0031 & 0 & 1 & 0 & 0 & 0.0031 \\ 0 & 0.0031 & 0 & 1 & 0 & 0 \\ 0 & 0 & 0 & 0 & 0 & 0 \\ 0 & 0 & 0 & 0 & 0 & 1 \end{bmatrix}$$

When the numerical values of the motor in Table I are substituted into the system, the following can be obtained:

$$\bar{A} = \begin{bmatrix} -64.5606 & -376.9911 & 965.3409 & 0 & 0 & 0 \\ 376.9911 & -64.5606 & 0 & 965.3409 & 0 & 0 \\ 0.0884 & 0 & -2.9556 & -376.9911 & 0 & 0 \\ 0 & 0.0884 & 376.9911 & -2.9556 & 0 & 0 \\ 0 & 0 & 0 & 0 & 0 & 0 \\ 0 & 0 & 0 & 0 & 0 & 0 \end{bmatrix}.$$

$$\bar{T}\bar{A} = \begin{bmatrix} -64.5606 & -376.9911 & 965.3409 & 0 & 0 & 0 \\ 376.9911 & -64.5606 & 0 & 965.3409 & 0 & 0 \\ -0.1093 & -1.1543 & 0 & -376.9911 & 0 & 0 \\ 1.1543 & -0.1093 & 376.9911 & 0 & 0 & 0 \\ 0 & 0 & 0 & 0 & 0 & 0 \\ 0 & 0 & 0 & 0 & 0 & 0 \end{bmatrix}.$$

A lower triangular matrix R with the same eigenvalues as $(\bar{T}\bar{A} - \bar{L}\bar{C})$ is considered, and the matrices $\bar{e}_1, \bar{e}_2$ satisfy Theorem 2. The eigenvalues of $(\bar{T}\bar{A} -$

$\bar{L}\bar{C}$) are -50.6767, -25.0914 ± 34.6127i, -36.5993 ± 27.4065i and -41.9045.

$$\bar{e}_1 = \begin{bmatrix} 1 & 8 & -2 & 1 & -2 & -1 \end{bmatrix}$$

$$\bar{e}_2 = \begin{bmatrix} 1 & 0 & 0 & 1 & 0 & -1 \end{bmatrix}$$

$$R = \begin{bmatrix} -50.6767 + 0.0000i & 0.0000 + 0.0000i & 0.0000 + 0.0000i \\ 1.0000 + 0.0000i & -25.0914 + 34.6127i & 0.0000 + 0.0000i \\ 1.0000 + 0.0000i & 1.0000 + 0.0000i & -25.0914 - 34.6127i \\ 1.0000 + 0.0000i & 1.0000 + 0.0000i & 1.0000 + 0.0000i \\ 1.0000 + 0.0000i & 1.0000 + 0.0000i & 1.0000 + 0.0000i \\ 1.0000 + 0.0000i & 1.0000 + 0.0000i & 1.0000 + 0.0000i \end{bmatrix}$$

$$\begin{bmatrix} 0.0000 + 0.0000i & 0.0000 + 0.0000i & 0.0000 + 0.0000i \\ 0.0000 + 0.0000i & 0.0000 + 0.0000i & 0.0000 + 0.0000i \\ 0.0000 + 0.0000i & 0.0000 + 0.0000i & 0.0000 + 0.0000i \\ -36.5993 + 27.4065i & 0.0000 + 0.0000i & 0.0000 + 0.0000i \\ 1.0000 + 0.0000i & -36.5993 + 27.4065i & 0.0000 + 0.0000i \\ 1.0000 + 0.0000i & 1.0000 + 0.0000i & -41.9045 \end{bmatrix}.$$

Then, the transformation matrix can be obtained by Theorem 2,

$$P = \begin{bmatrix} -50.6767 - 0.0000i & 0.0000 - 0.0000i & 0.0000 - 0.0000i \\ 0.9999 - 0.0001i & -25.0914 + 34.6127i & 0.0000 - 0.0000i \\ 1.0000 - 0.0006i & 1.0000 + 0.0001i & -25.0914 - 34.6127i \\ 1.0000 - 0.0000i & 1.0000 + 0.0000i & 1.0000 - 0.0000i \\ 0.9999 + 0.0005i & 1.0001 - 0.0001i & 1.0000 + 0.0000i \\ 1.0001 - 0.0000i & 1.0000 - 0.0000i & 1.0000 - 0.0000i \end{bmatrix}$$
$$\begin{bmatrix} 0.0001 + 0.0001i & 0.0000 - 0.0000i & 0.0000 + 0.0000i \\ 0.0001 - 0.0004i & 0.0000 + 0.0000i & 0.0000 + 0.0000i \\ 0.0011 - 0.0011i & 0.0000 + 0.0000i & 0.0000 + 0.0001i \\ -36.5993 + 27.4065i & 0.0000 - 0.0000i & 0.0000 + 0.0000i \\ 0.9989 + 0.0006i & -36.5993 - 27.4065i & 0.0000 - 0.001i \\ 1.0001 + 0.0001i & 1.0000 - 0.0000i & -41.9045 + 0.0000i \end{bmatrix}.$$

Matrix P is proved to be nonsingular, and the simulation results are displayed as follows. Figure 1 illustrates the fault estimation response with the region pole placement. The simulation results show that the fault estimate curve finally tracks the actual failure, and the real fault is between the upper bound fault observation value and the lower bound observation value.

Figure 2 shows the fault estimation response without region pole placement. The fault tracking speed in Figure 1 is faster than in Figure 2. Thus, the performance of the fault estimation can be improved after considering a circular domain constraint to the solution.

Part 2. The method mentioned in subsection 3.3 will be validated in this subsection. Firstly, we study the influence of the numerical value of the parameter l_{61} on the interval size when other parameters remain unchanged. The simulation results are as follows. The small figure inside Figure 3 is the locally enlarged figure. Figure 3 shows that the interval size decreases with the decrease of the parameter l_{61}. Hence, the smaller the parameter l_{61}, the better the effect of fault estimation will be. Next, we study the influence of the numerical value

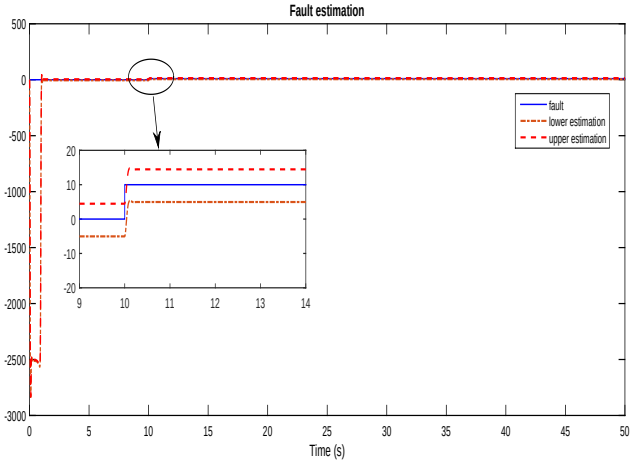

Figure 1: Simulation results with region pole placement.

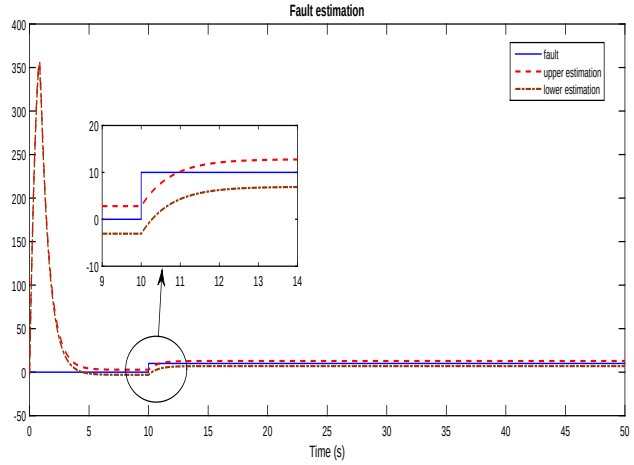

Figure 2: Simulation results without region pole placement.

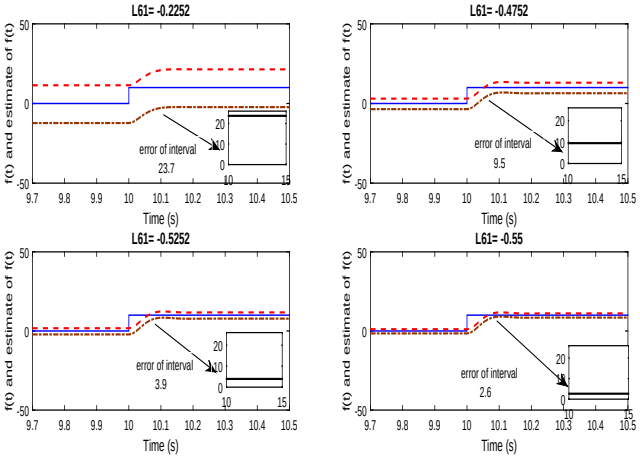

Figure 3: Simulation results with different parameter L_{61}.

of the parameter l_{62} on the interval size when the other parameters remain unchanged. The simulation results are as follows, in which, the small figure inside

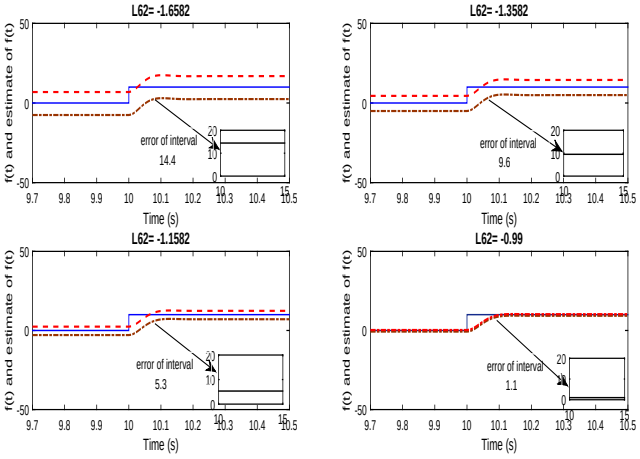

Figure 4: Simulation results with different parameter L_{62}.

the figure 4 is error of the upper and lower bounds. Figure 4illustrates that the interval size decreases with increase in parameter l_{61}. Therefore, the bigger the parameter l_{62}, the better the effect of fault estimation will be.

5. Conclusion

In this paper, an IO-UIO based fault estimation scheme for high-speed railway traction devices with sensor fault and disturbances is investigated. For the nonlinear part of the system, an interval observer is introduced to solve efficiently only a part of the information in the interval. Therefore the design of unknown input observer is proposed, and this parameter can completely eliminate the external disturbance. Moreover, an FD algorithm is proposed to estimate the faults accompanied by disturbance. We constructed a Metzler matrix to match the properties of the interval observers by transforming the coordinates. In addition, we found a performance index that can adjust the size of the interval observer. Finally, the effectiveness and advantages of the proposed IO-UIO method for high-speed railway traction devices is shown through simulation results.

References

[1] Y. J. Wang, Impediment to progress and inevitable trend of the high-speed railway development in china, (15) (2014) 256–258.

[2] S. Peng, R. Agarwal, Robust disturbance attenuation for discrete-time active fault tolerant control systems with uncertainties, in: Guidance, Navigation, and Control Conference and Exhibit, 1999.

[3] S. Y. Han, Y. H. Chen, G. Y. Tang, Fault diagnosis and fault-tolerant tracking control for discrete-time systems with faults and delays in actuator and measurement, Journal of the Franklin Institute.

[4] Hu, Xiao, Friswell, M.I, Robust fault-tolerant control for spacecraft attitude stabilisation subject to input saturation, Control Theory & Applications Iet 5 (2) (2011) 271–282.

[5] Q. Hu, B. Xiao, Y. Zhang, Fault-tolerant attitude control for spacecraft under loss of actuator effectiveness, Control & Decision 34 (3) (2015) 263–268.

[6] L. Wu, X. Yao, W. X. Zheng, Generalized h2 fault detection for two-dimensional markovian jump systems, Automatica 48 (8) (2012) 1741–1750.

[7] X. Ding, P. M. Frank, Fault detection via factorization approach, Systems & Control Letters 14 (5) (1990) 431–436.

[8] P. Shi, M. Liu, L. Zhang, Fault-tolerant sliding-mode-observer synthesis of markovian jump systems using quantized measurements, IEEE Transactions on Industrial Electronics 62 (9) (2015) 5910–5918.

[9] W. Chen, M. Saif, A sliding mode observer-based strategy for fault detection, solation, and estimation in a class of lipschitz nonlinear systems, International Journal of Systems Science 38 (12) (2007) 943–955.

[10] G. X. Zhong, G. H. Yang, Fault detection for discrete-time switched systems with sensor stuck faults and servo inputs, Isa Transactions 58 (2015) 196–205.

[11] D. Hu, A. Sarosh, Y. F. Dong, A novel kfcm based fault diagnosis method for unknown faults in satellite reaction wheels., Isa Transactions 51 (2) (2012) 309–316.

[12] T. A. Nakamura, R. M. Palhares, W. M. Caminhas, B. R. Menezes, M. C. M. M. D. Campos, U. Fumega, C. H. D. M. Bomfim, A. P. Lemos, Adaptive fault detection and diagnosis using parsimonious gaussian mixture models trained with distributed computing techniques, Journal of the Franklin Institute 354 (6).

[13] C. Liu, B. Jiang, K. Zhang, Incipient Fault Detection Using an Associated Adaptive and Sliding-Mode Observer for Quadrotor Helicopter Attitude Control Systems, Birkhauser Boston Inc., 2016.

[14] S. Zhang, K. R. Pattipati, Z. Hu, X. Wen, C. Sankavaram, Dynamic coupled fault diagnosis with propagation and observation delays, IEEE Transactions on Systems Man & Cybernetics Part B 43 (6) (2013) 1424–1439.

[15] H. Dong, Z. Wang, J. Lam, H. Gao, Fuzzy-model-based robust fault detection with stochastic mixed time delays and successive packet dropouts, IEEE Transactions on Systems Man & Cybernetics Part B Cybernetics A Publication of the IEEE Systems Man & Cybernetics Society 42 (2) (2012) 365.

[16] S. Tong, L. Zhang, Y. Li, Observed-based adaptive fuzzy decentralized tracking control for switched uncertain nonlinear large-scale systems with dead zones, IEEE Transactions on Systems Man & Cybernetics Systems 46 (1) (2015) 37–47.

[17] H. H. T. Liu, P. Shi, B. Jiang, Fault detection, diagnosis, and fault tolerant control with flight applications, Journal of the Franklin Institute 350 (9) (2013) 2371–2372.

[18] X. G. Yan, C. Edwards, Robust sliding mode observer-based actuator fault detection and isolation for a class of nonlinear systems, in: Decision and Control, 2005 and 2005 European Control Conference. Cdc-Ecc '05. IEEE Conference on, 2005, pp. 987 – 992.

[19] T. Wang, W. Xie, Y. Zhang, Sliding mode fault tolerant control dealing with modeling uncertainties and actuator faults, Isa Transactions 51 (3) (2012) 386.

[20] L. Qin, X. He, R. Yan, R. Deng, D. Zhou, Distributed sensor fault diagnosis for a formation of multi-vehicle systems , Journal of the Franklin Institute.

[21] Z. Iwai, M. Sato, A. Inoue, K. Mano, An adaptive observer with exponential rate of convergence, Transactions of the Society of Instrument & Control Engineers 18 (4) (2009) 343–348.

[22] S. Roy, I. N. Kar, Adaptive sliding mode control of a class of nonlinear systems with artificial delay, Journal of the Franklin Institute.

[23] M. Chen, P. Shi, C. C. Lim, Adaptive neural fault-tolerant control of a 3-dof model helicopter system, IEEE Transactions on Systems Man & Cybernetics Systems 46 (2) (2016) 260–270.

[24] X. G. Yan, C. Edwards, Adaptive sliding-mode-observer-based fault reconstruction for nonlinear systems with parametric uncertainties, IEEE Transactions on Industrial Electronics 55 (11) (2008) 4029–4036.

[25] K. Zhang, V. Cocquempot, B. Jiang, Adjustable parameter-based multiobjective fault estimation observer design for continuous-time/discrete-time dynamic systems, International Journal of Control Automation & Systems 15 (3) (2017) 1077–1088.

[26] Y. Wu, B. Jiang, N. Lu, H. Yang, Y. Zhou, Multiple incipient sensor faults diagnosis with application to high-speed railway traction devices., Isa Transactions 67.

[27] Y. M. Fu, G. R. Duan, S. M. Song, Design of unknown input observer for linear time-delay systems, International Journal of Control Automation & Systems 2 (4) (2004) 530–535.

[28] D. Bestle, M. Zeitz, Canonical form observer design for non-linear time-variable systems, International Journal of Control 38 (2) (1983) 419–431.

[29] D. Efimov, T. Raissi, A. Zolghadri, Control of nonlinear and lpv systems: Interval observer-based framework, IEEE Transactions on Automatic Control 58 (3) (2013) 773–778.

[30] F. Mazenc, O. Bernard, Interval observers for linear time-invariant systems with disturbances , Automatica 47 (1) (2011) 140–147.

[31] F. Mazenc, T. N. Dinh, S. I. Niculescu, Interval observers for discrete-time systems, International Journal of Robust & Nonlinear Control 24 (17) (2015) 2867–2890.

[32] D. Efimov, W. Perruquetti, T. Rassi, A. Zolghadri, Interval observers for time-varying discrete-time systems, IEEE Transactions on Automatic Control 58 (12) (2013) 3218–3224.

[33] Y. G., Observer-based fault detection for induction motors, Masters Abstracts International 45 (3).